Design for Advanced Test and Safety for Image and Photonic Sensors

Julia Lefèvre, Philippe Debaud, Arnaud Virazel, Patrick Girard

Design for Advanced Test and Safety for Image and Photonic Sensors

J. Lefevre [1, 2] P. Debaud [1] P. Girard [2] A. Virazel [2]

[1] STMicroelectronics
Imaging division, DFT
Grenoble, France
julia.lefevre@st.com, philippe.debaud@st.com

[2] LIRMM
University of Montpellier / CNRS
Montpellier, France
<lastname>@lirmm.fr

I. Motivation and Problems

A. Context and Problem Statement

Nowadays, **C**MOS **I**mage **S**ensors (CIS) can be found everywhere, e.g., in smartphones, autonomous cars or night vision systems. A CIS is used to convert a physical phenomenon into an electrical signal. Basically, a light illumination made of photons is translated into an image made of pixel values. The general architecture of a CIS is split into optical and electrical elements. The optical element is a pixel array which translates the light information into an electrical information. The electrical elements can be ADCs or amplifiers and are used to translate and to convey the electrical information.

Irrespective of the application field, it is mandatory to test all the sensors to ensure that they all meet standard requirements. To do so, CIS testing is done at various stages of a sensor life, from characterization of the die on the wafer to online test of the sensor. Test of a CIS comprises electrical and optical tests, all usually performed on an ATE (**A**utomatic **T**est **E**quipment), in order to test all the elements inside the sensor. When one test fails (optical or electrical), the sensor is declared as defective and is withdrawn from the production line. The resulting test data is saved into a **S**tandard **T**est **D**ata **F**ormat (STDF) file [1].

Electrical tests can be functional, structural, or parametric depending on the part of the circuit (analog, digital or mix) which is under test [2].

Optical tests are performed thanks to image processing algorithms applied on the output images of the CIS under test. Typical image processing algorithms are 2D median filter and 2D convolution [3]. Results of these optical tests allow to check if output images are correct according to predefined image quality metrics [4]. During optical testing, the CIS under test is put in different states (**dark or light** illuminations and **short or long** integration times) to verify its correct operation in a wide variety of conditions.

Usually, it is necessary to wait for several images to be captured entirely and stored in a memory by the ATE before computing metrics and determine if the sensor images pass the optical tests or not. This mean that test time and data storage dedicated to test may become prohibitive, e.g. test time can go from 10 seconds to 1 minute which can represent up to 30% of the final product cost [5-6].

B. State of the Art in CIS Testing

In the literature, some solutions have been proposed to embed test facilities (BIST, **B**uilt-**I**n **S**elf-**T**est) inside a CIS and hence save test time by reducing optical test time. Authors in [6-8] and in [9-10] propose to reduce the amount of optical tests and proceed with a fully electrical test set so as to avoid precise and restrictive settings needed in optical tests.

Authors in [6-7] propose a solution based on the generation of a pulse (voltage stimuli) which is sent on the anode of the photodiode inside the pixel to simulate the light illumination. Authors indicate that the implementation of this method is very dependent on the pixel architecture. This structural-based test is done on the pixels of the array independently of each other, without any management of clustering pixels. Experimental results demonstrate a relatively good correlation in dark conditions with respect to tests performed with an ATE, but the comparison is unreliable in the light conditions due to the use of a light source not stable enough.

The work presented in [8-9] proposes a BIST framework to detect defective lines used to read out or addressing pixels, thanks to the extraction of the impedance of lines. Authors use two solutions for the detection of continuous and partial defective lines. One solution deals with continuous defective lines by reusing the ADC circuitry to measure resistances. The other solution uses a vector network analyzer equipment to drive the RF impedance used to detect partial defective lines. Despite its efficiency, this solution needs additionnal equipment (line delay detector, delay controler, pulse detector, etc.) to detect defective lines.

C. Objectives

The work developed during this PhD is intended to be used at a production test level in order to sort out *PASS* and *FAIL* sensor dies. The strategy consists of three different and independent BIST solutions to screen out optical defects.

The main objective is to reduce the significant CIS test time required by typical external test procedures at a low cost.

By transforming two-dimensional computations into one-dimensional, at-speed computations realized inside the sensor, test complexity and test data storage requirements are limited, and test time is saved.

II. Scientific and Technological Excellence of the Work

During this PhD, we developed three different BIST solutions aimed at reducing the optical test time. The three BIST solutions presented in this section are fully digital and are split into hardware and software parts to perform a functional test of the optical elements of the CIS under test. The input of each BIST is the 1D flow of digital pixel values coming from the pixel array. The outputs of each BIST are a *PASS*/*FAIL* information (a.k.a *PASS*/*FAIL* **label**) related to the CIS under test as well as the number of singlets, couplets and cluster associated to each image with the defects location.

A defect is a deviation from the specification. A certain pixel value is expected in precise conditions (*i.e.*, illumination or integration time). Nevertheless, a range around the admissible pixel value (more or less a few gap) is allowed due to the presence of noise. The pixel value which is too distant from the expected value is defined as a defective pixel.

In this work, we distinguish local defects from global defects. A local defect is located in a A*A kernel of pixels (containing A^2 pixels, with "A" an odd integer). A singlet (i.e., one defective pixel in A*A), a couplet (i.e., two defective pixels in A*A) or a cluster (i.e., more than three defective pixels in A*A) are 3 kinds of local defects. A global defect affects a large pixel area. Defective row or column are two examples of global defects. A certain number of singlets or couplets is admissible below a certain limit whereas the presence of a cluster or a global defect are not admissible.

A. *PETS BIST Solution [10-11]*

a) Concept and Approach

To deal with output images provided by a CIS, PETS BIST solution reuses the way pixels are scanned in conventional image processing algorithms (convolution and median filtering) applied with an ATE. Owing to several parameters used to define defects such as defective pixel or defective row inside the pixel array, PETS BIST is able to sort out good and bad sensors.

To test the pixel array, the BIST engine needs to access each arithmetic pixel value inside the array. The array is streamed row by row at the pixel rate thanks a sequencer block which controls the system in conjunction with an external clock. When a pixel is dealt with the BIST module, first, the pixel type (Red, Green, Blue or monochrome) is determined from the pixel coordinates. Then, the arithmetic value of the pixel is compared with two thresholds computed from a local average. If the pixel value is outside the defined range, the pixel is defective and its data (value and coordinates) are stored in a memory for the next phase. Otherwise, these data are not saved.

Once all the pixels of the array have been evaluated by PETS BIST, the data of each defective pixels stored inside a memory is read by a software program which is able to count singlets, couplets and determine whether there is a cluster or not into the pixel array of the CIS under test.

The PETS BIST solution has been implemented in Verilog language. The proposed PETS BIST architecture is depicted in Fig. 1 where each digital block is dedicated to one function.

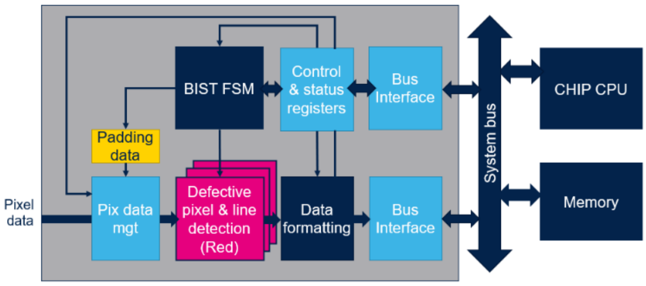

Figure 1: General PETS BIST architecture

All the blocks detailed in this architecture are synchronized by a Finite State Machine (*BIST FSM*) which is used to manage the BIST process by launching appropriate signals and collecting required information. Communications between the various blocks is done owing to wires (1-bit signal carriers) or bus (word of several bits carrier).

In order to test all pixels in a CIS array, each pixel is selected based on its type (red, green or blue) since a pixel of one type can only be tagged as defective with respect to pixels of the same type. The block *Pixel data mgt* guides the pixel in dedicated accumulators located inside the *Defective pixel & line detection* block to store pixel values of the same type. This allows to do parallel computations on several accumulators to pipeline the detection on several pixel types.

If a pixel is located near the borders of the array, it is mandatory to compute a padding value to detect if the pixel is defective or not. This suggests a coordinate management inside the BIST module, that can be done with counters operating at the pixel rate and returning row and column relative positions in the array.

Then, the pixel is processed by the *Defective pixel & line detection* block. More precisely, the value of the pixel is compared to thresholds to determine if the pixel is correct or defective. The pixel data, i.e. the value of the pixel, its coordinates and its type, are stored in the memory of the sensor in case it is declared as defective.

The information "the pixel is defective" in the form of a boolean will launch the writing of the pixel data inside the external memory. Note that, to avoid test hardware overhead, the external memory is a memory already existing in the CIS but not used during the test phase and hence available to store pixel data of defective pixels. The coordinates and values of a defective pixel are encoded by the *Data formatting* block before storage in the memory.

b) Obtained Results

Performances of our solution have been evaluated owing to a software emulation of the developed BIST engine.

The validation of PETS BIST is based on maximizing correlation and minimizing the number of misclassified images. The correlation is a high level information that quantifies the similarities between the ATE-based optical tests and BIST-based tests. The correlation is achieved by comparing the STDF label and the BIST label of the different groups of image types (*i.e.*, illumination and integration time conditions). These correlations are expressed in percentage.

In order to validate PETS BIST solution, we performed experiments by using two databases (DBs) composed of images taken by CISs in dark and light environments for short and long integration times. The goal of our experiments is to demonstrate the efficiency of the BIST solution in reproducing part of optical tests for CIS as they are usually applied with an ATE.

A first DB (called DB1 in the following) composed of output images coming from more than 2,400 CISs originating from the same packet were used in our experiments. Each packet is a set of sensors that have been manufactured on the same production chain. Among these 2,400 CISs, a part of them were identified as *FAIL* by former ATE-based optical tests. Images coming from these CISs were selected so as to get a representative sample of various defect categories, i.e., singlets, couplets, defective columns, defective rows, clusters of various sizes, etc. For each CIS, we collected the **same number** of dark and light images so that the dataset was split into two equivalent sets of dark and light images as shown in Fig. 2.

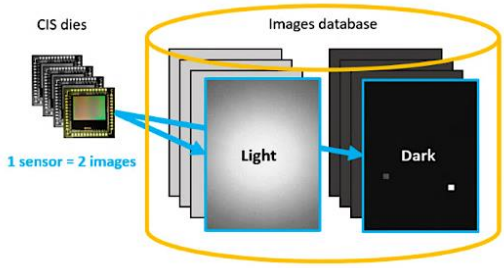

Figure 2: Data Distribution of DB1 [12]

A second DB (called DB2 in the following) is used to validate the efficiency and hence generalize the use of PETS BIST solution over different sensors. This section presents the results obtained by using the BIST solution for a package of 28,000 images with the final goal to reach remaining **P**art **P**er **M**illion (ppm) results.

Similarly to DB1 (see Fig. 2), the organisation of DB2 contains images and STDF file for a package of approximately 7,000 sensors (i.e., 28,000 images). As shown in Fig. 3, the output images of DB2 are split into dark and light images, i.e. both using long and short capture times, one CIS of DB2 gives four images instead of two in DB1.

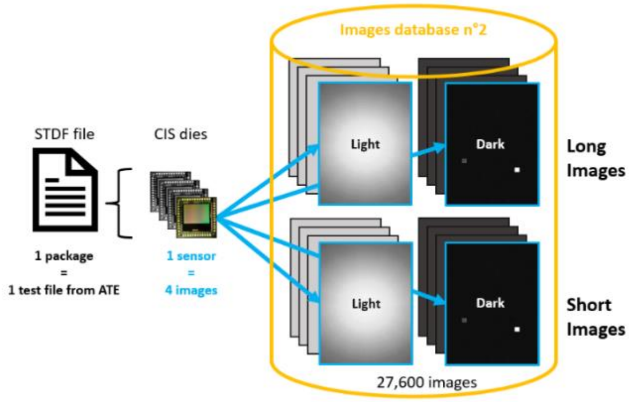

Figure 3: Data Distribution of DB2 [13]

The subset of images coming from the *FAIL* CISs was organized into several categories with respect to the defect type. For each image, the numbers of singlets and couplets are known, as well as the presence of cluster, thanks to the output data from former optical tests performed on ATE.

Several steps are necessary to set up the appropriate BIST parameters (the thresholds). The PETS BIST parameters are chosen empirically and are dependent to the DB and the CIS under test.

Table I summarizes the results obtained by applying PETS BIST to perform optical test of CIS from DB1 and DB2. The correlation between the results obtained by the ATE and those obtained by PETS BIST are 99.95% and 99.64%, respectively.

TABLE I. SUMMARY OF PETS BIST RESULTS [11-12] WITH NUMBER OF CISS IN THE DB (NB CIS), NUMBER OF IMAGES IN THE DB (NB IMG), CORRELATION IN % AND MAIN MISCLASSIFICATION CAUSE

DB	Nb CIS	Nb Img	Correlation (%)	Misclassification Cause
DB1	2,400	4,800	99.95	1 small cluster missed by PETS BIST
DB2	6,900	27,600	99.64	Defective columns missed by PETS BIST

For DB1, the study of the 0.05% misclassifications shows that the setting used for PETS BIST do not allow for the detection of one small cluster in one image. After visual analysis, it was determined that this cluster is not a significant element that could greatly degrade the quality of the test image.

For DB2, the study of the 0.36% misclassifications revealed a few missed defective columns by PETS BIST for a given setting.

Similarly to DB1, visual analysis shows that the missed defective columns from the misclassified images in DB2 are specific. For a given image, the difference in values between the missed defective column and its neighboring columns is very slight. Therefore, the values of the missed defective columns have a slightly variation compared to the values of the other columns. This limitation of PETS BIST was expected since, by nature, PETS BIST is based on horizontal detection. Addressing this aspect would require adding more hardware and increasing the complexity of PETS BIST.

c) Novelty and Foundational Character

The area overhead required by the BIST hardware limits the amount and complexity of possible computations, so that embedding conventional image processing algorithms used for optical test in a BIST engine can be too costly. Indeed, convolution and filtering methods used in image processing algorithms are generally based on **two-dimensional** data that are available when an entire image has been stored. However, when only a flow of pixels coming from a row of the pixel array is available, using such methods becomes impossible.

To alleviate this issue, the novelty of PETS BIST is to reuse the way pixels are scanned in 2D convolution and 2D median filtering methods to deal with **1D row of pixels**. With this modification, we avoid the need of additional hardware to store data during the reading of the array, and we limit the complexity of operations that are specific to 2D data management, thus reducing test time.

The proposed PETS BIST engine does not embed all optical tests usually performed on an ATE. Compared to existing BIST approaches from the literature, the advantages of PETS BIST solution are that i) it represents less than a few percents of the total CIS area, far below what can be achieved with some of the existing solutions, and ii) all potential local defects in the pixel array can be detected, while only a part of them are covered by existing BIST solutions.

B. *PRED BIST Solution [14]*

a) Concept and Approach

The human eye is very sensitive to global variations. For example, a "huge" defect inside an image (*i.e.*, a defect affecting a significant group of pixels) will easily be found while a single defective pixel will not be. A human considers the homogeneity of the entire image as a key point to decide if it is a good or a bad image.

PRED BIST solution still has the same objective as PETS BIST, *i.e.*, to reduce the optical test time. Its main difference is based on a global overview of the image (as a human would do), which handles an image as a continuous mesh of pixel values.

Operating PRED BIST is done in three phases that require to read the pixel array twice: a first time to read and select samples (i.e. reference points) inside the image (a.k.a. phase 1), and a second one to build the ideal image and to compare the ideal and the real images (phase 2 and 3 simultaneously). PRED BIST computes an ideal image from each output image of the CIS under test owing to an arithmetic method (*i.e.*, bilinear interpolation). The ideal image is then compared to the real image during phase 3. Offsets are added to the ideal image to perform the comparison since, during the real CIS operation, the image never totally matches the ideal image. These offsets create an envelope defining the correct pixel values and this envelope depends on the so-called x parameter.

PRED BIST detects all global defects (*i.e.*, defective row or column, noise presence, etc.) and is also able to catch local defects such as singlets, couplets, etc.

The CIS die sorting is done by resorting to two types of resources: i) the BIST infrastructure embedded in the CIS for test and defective pixel detection, and ii) two external memories for test data storage. This distribution of tasks has been decided to achieve the best trade-off between test time efficiency and CIS hardware overhead. The CHIP CPU is used for defect classification. One important point is the location of the BIST module inside the CIS architecture. In order to avoid pre-processing on pixel values, that could potentially correct and hide potential defects, pixel values must come directly from the pixel array without going through intermediate hardware modules. The general BIST architecture is depicted in Fig. 4 where each digital block is dedicated to one function. This solution has been implemented in Verilog language.

In order to test all pixels in a CIS array, each pixel is selected based on its type (Red, Green, Blue or monocolor) . The block *Pixel data management* ("Pix data mgt" block in Fig. 4) allows to select the pixels of the same color using to the coordinates of the current pixel.

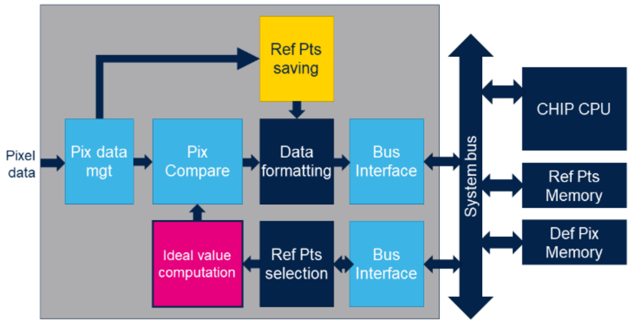

Figure 4: General PRED BIST Architecture

During Phase 1 (*i.e.*, Selection of Reference Points), the pixel array is streamed and the *Reference Points saving* block ("Ref Pts saving") selects all the reference points. The data of the reference points (*i.e.*, pixel values and coordinates) is saved into the *Reference Points Memory* ("Ref Pts Memory"). The pixel array is streamed again and the *Reference Points Memory* is accessed by the *Reference Points Selection* block ("Ref Pts selection") in order to get back the four corresponding reference points thanks to the coordinates of the PUT (**P**ixel **U**nder **T**est). The values of the four reference points are used to compute the ideal value of the PUT by the *Ideal Value Computation* block (Phase 2). Then, the *Pixel Compare* block builds the envelope that depends on the x parameter and makes a comparison between the real values and the envelope (Phase 3). The 3D representation of the envelope, computed from the ideal values, is given in grey in Fig. 5. The real values are represented in blue in Fig.5.

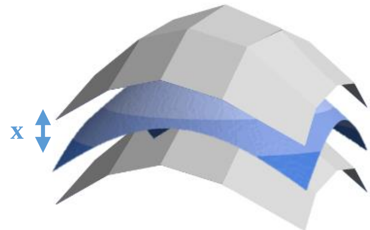

Figure 5: 3D Representation of the Real Image in Blue and the Envelope in Grey computed from the Ideal Image

If the pixel value is outside the envelope, the data of the pixel is formatted by the *Data Formatting* block and saved into the *Defective Pixel Memory* ("Def Pix Memory"). This memory will be read by a program embedded on the Chip CPU to classify the defective pixels into singlets, couplets or cluster. The program is also able to give the *PASS*/*FAIL* label from the number of defects.

b) Obtained Results

DB2 (an extract of which had already been used for PETS BIST validation), is composed of output images coming from more than 11,450 monocolor CISs originating from different packets, were used in our experiments. Among these 11,450 CISs, a part of them were identified as *FAIL* by former ATE-based optical tests. For each CIS, we collected the same number of Dark and Light images so that the DB was split into two equivalent sets of Dark (Short and Long) and Light (Short and Long) images as shown in Fig. 2.

Another DB, called DB3, is composed of output images coming from 20,460 RGB CISs and is illustrated in Fig. 6.

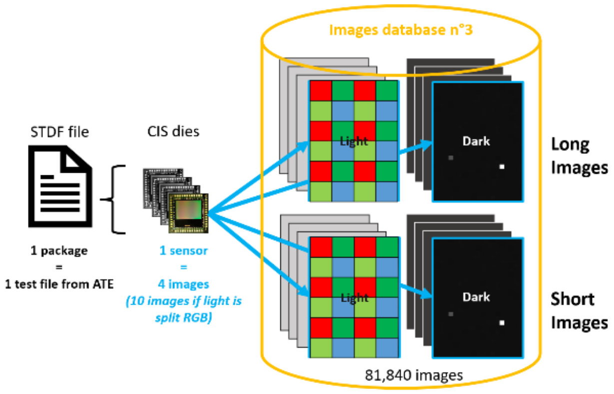

Figure 6: Data Distribution of DB3

One CIS gives 10 images if the Light image is split into Red, Green1, Green2 and Blue images. To split Light images, pixels of the same color are joined together inside a new image with a lower size than the original one.

The subset of images coming from *FAIL* CISs was organized into several categories with respect to the defect type. For each image, the number of singlets and couplets is known, as well as the presence of clusters (*i.e.*, group of defective pixels, defective rows or columns, wave, etc.), thanks to the output data from former ATE-based optical tests (data available into STDF files).

Moreover, we have to calibrate the x parameter used to set the envelope for each type of sensor (*i.e.*, monocolor or RGB). The x parameters have been selected experimentally to achieve the best trade-off between the admissible number of defective pixels inside all images and the minimization of the number of misclassified images compared to the ATE-based optical tests. The x parameters are calibrated separately depending on DB2 and DB3.

The sensors used to build DB2 and DB3 come from different packets of sensors. By this way, a significant number of sensors from different manufacturing conditions can be considered in our experiments. In fact, all the production chains used during manufacturing stage are different due to potential process deviations or difference of settings. Experimental results presented bellow consider each DB as a unique set of sensor images coming from the sum of all the packets.

Table II summarizes the results obtained by applying PRED BIST to perform optical test of CIS from DB1 and DB2. The correlation between the results obtained by the ATE and those obtained by PRED BIST are 99.90% and 99.40%, respectively.

TABLE II. SUMMARY OF PRED BIST RESULTS [15] WITH NUMBER OF CISS IN THE DB (NB CIS), NUMBER OF IMAGES IN THE DB (NB IMG), CORRELATION IN % AND MAIN MISCLASSIFICATION CAUSE

DB	Nb CIS	Nb Img	Correlation (%)	Misclassification Cause
DB2	11,450	45,800	99.90	Triplet found in excess by PRED BIST
DB3	20,460	81,840	99.40	Couplet missed by PRED BIST

For DB2, the study of the 0.10% misclassifications shows that PRED BIST tends to reject additional CISs. The BIST identified that these CISs have the characteristic of containing triplets (3 defective pixels in an A*A kernel of pixels) while the ATE considered that there were none. However, after visual analysis, these triplets can be easily identified manually and could potentially cause problems in the output images of the sensor. Therefore, with a chosen setting, PRED BIST is stricter than the optical tests launched on the tester. Additionally, PRED BIST will not miss any defects since 100% of the misclassifications come from defects found by the BIST for DB2.

Compared to the results of PETS BIST on the same DB, the correlation between the PRED BIST results and the ATE-based results is 0.26% higher than the correlation between the PETS BIST results and the ATE-based results. Additionally, PETS BIST tended to miss critical defects such as defective columns, while PRED BIST is stricter than the optical tests currently used on ATE and do not miss any critical defect.

For DB3, the study of the 0.60% misclassifications revealed a few missed defective columns by PETS BIST for a given setting. Figure 7 gives the distribution of the misclassifications causes from the 0.60% misclassifications.

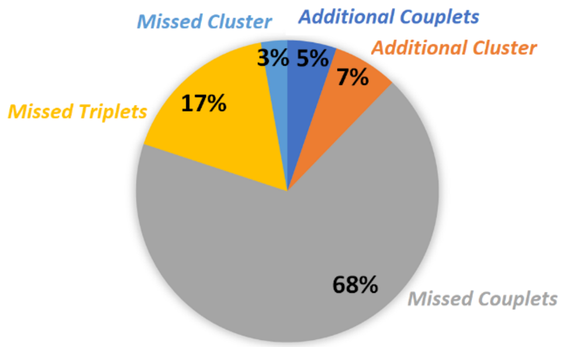

Figure 7: Distribution of Misclassification Causes on using PRED BIST for DB3 Optical Test

The misclassification causes are split into missed defects, which represent 88% of the misclassifications (coupMiss 68%, tripMiss 17% and clusMiss 3%), and defects found in excess (*i.e.*, defects found by PRED BIST and not by ATE-based optical tests, coupOnly 5% and clusOnly 7%), which represents 12% of the misclassifications. The major part of the misclassified images are images with couplets missed by PRED BIST. The missed couplets and triplets are local defects that can be subject to discussion. In fact, a difference of few pixel values can be difficult to detect if the x parameter used to set up the envelope is not well chosen. Moreover, if the x parameter varies, one pixel of the couplet can toggle from correct to defective, or vice-versa. During the test, PRED BIST is able to find one of the defective pixel forming the couplet but may not find the other defective pixels of the couplet, so it classifies the defect as a simple singlet, unlike what would be done by an ATE-based optical test.

PRED BIST finds that 5% of the misclassified images have too many couplets compared to the couplets limit and 7% of the misclassified images have a cluster whereas the ATE-based optical tests do not find any issues inside the images (or find a number of couplets bellow the admissible couplets limit). After visually studying the misclassified images, the visual analysis allows us to classify them as *FAIL* due to some visible breaks in the uniformity. This means that the calibration of PRED BIST are stricter than the calibration of ATE-based optical tests. With PRED BIST calibration, it is possible to reach a higher accuracy compared to the tolerances currently accepted in production. In fact, the calibration of the optical tests performed with an ATE is chosen in order to let pass images with specific defects, considered as admissible.

An important defect type that should not be left behind by PRED BIST is a cluster. The visual study of the images (3% of the misclassifications as reported in Fig. 7) shows that the missed cluster corresponds to a local group of few defective pixels (*i.e.*, more than three defective pixels) with a slight difference of pixel values compared to the values inside the A*A kernel of pixels. No defective row or column, i.e., global defects, are missed by PRED BIST. This is an important information since it is not admissible to miss one or several global defects inside the image.

As for PETS BIST, addressing the fact that PRED BIST misses some local defects would require adding more hardware and increasing the complexity of PETS BIST.

c) Novelty and Foundational Character

The novelty of the approach relies on the ability to predict a ideal image from each output image of the CIS without the need to launch external optical tests performed with an ATE.

Unlike PETS BIST that still requires the use of an external test to detect global defects, all optical algorithms usually applied by an ATE are covered by the use of PRED BIST, making this solution an “all-in-one” test solution. It results in a reduction of up to 95% of the optical test time. Moreover, PRED BIST avoids the storage of full images as it only needs to save few pixel values inside the image.

C. *HYBRID BIST Solution*

a) Concept and Approach

The concept of this third BIST solution is to combine the advantages of the previously presented PETS and PRED solutions to create a single solution that mixes the two solutions. The idea is to use the precise local defect detection capability of PETS BIST and the precise global defect detection capability of PRED BIST.

As the creation of this latest BIST solution is relatively recent, several questions arise when combining the two previous BIST techniques. If they are to be launched sequentially, it is possible to optimize the test time by stopping the test if the sensor is found to be defective by the first BIST, without launching the second BIST (GoNoGo test). Launching the two BIST sequentially would be much longer and less efficient because between each BIST launching, the results found by the first BIST would need to be analyzed before launching the second BIST.

If the two BIST are launched in parallel, it is necessary to manage the duplicate defective pixels to avoid storing unnecessary test information.

Calibration is also an important consideration because the two BIST are calibrated independently due to their different operating principles. Therefore, it will be necessary to apply a parameter for each BIST. Finding the right setting for HYBRID BIST will involve seeking for balance between the two parameters.

b) Obtained Results

The HYBRID BIST solution has not yet been implemented in Verilog like PETS BIST and PRED BIST. We only have the software emulation of HYBRID BIST to acquire the first results.

For the preliminary architecture of HYBRID BIST, it is important to consider the common blocks between the two BIST solutions to avoid unnecessary space loss. A first architecture was proposed theoretically by combining the two BIST solutions without optimization (*i.e.*, without combining the common blocks). This architecture will be improved in the future. The graph in Fig. 8 provides a comparison of the percentage representations of PETS BIST (in orange), PRED BIST (in blue), and HYBRID BIST (in green) based on the total size of ten monochrome sensors from the smallest (on the left) to the largest (on the right).

As mentioned earlier, the green curve in Fig. 8 represents the worst possible case for the implementation of HYBRID BIST since this theoretical architecture considers it as the sum of PETS BIST and PRED BIST, rather than a complementary set containing shared digital blocks.

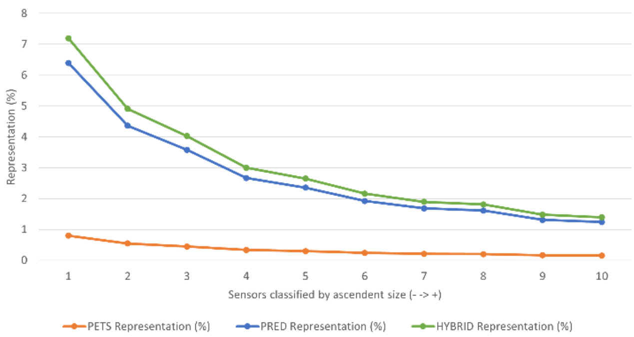

Figure 8: BIST Area overhead Representation in % versus the Total Sensor Area for 10 Different Monocolor CISs (little CIS on the left and big CIS on the right)

Thus, we can see that the impact of adding PETS BIST to PRED BIST is relatively low, as the difference between “only PRED BIST use” and “HYBRID BIST use” is 0.80% for a small sensor and 0.15% for a large sensor. Therefore, it would be interesting to implement HYBRID BIST, which represents between 1.4% and 7.2% of the total size of CISs in Fig. 8, in the case of optical test of large sensors (1.4% of the total size).

As the analysis of HYBRID BIST results is time-consuming due to the need to consider several parameter pairs to minimize the number of misclassified images, it is currently only possible to provide results for DB3 for three subpackages containing approximately 9,700 images, 38,000 images and 34,100 images, respectively.

The graph in Fig. 9 shows the evolution of correlations before (blue curve) and after (orange curve) the addition of PETS BIST to PRED BIST, sequentially for a manually chosen calibration.

The preliminary study depicted in Fig. 9 demonstrates that HYBRID BIST will reduce the number of misclassified images and, consequently, the number of misclassified sensors. Specifically, for the three sub-packages of DB3, the correlation increases from 99.64% to 99.69% for sub-package 1 (+0.05%), from 99.68% to 99.72% for sub-package 2 (+0.04%), and from 99.67% to 99.73% (+0.06%) for sub-package 3.

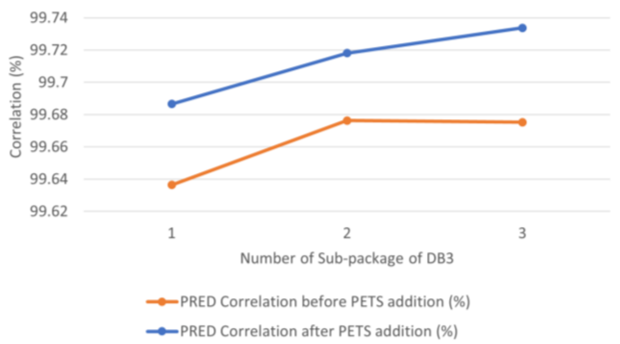

Figure 9: Correlations for Three sub-packages of DB3 before (blue) and after (orange) Addition of PETS BIST to PRED BIST use

To validate HYBRID BIST, the upcoming study will present results for an appropriate combination of PRED BIST and PETS BIST (without sequential launching). Additionally, future experiments will be conducted on other types of sensors to further validate the HYBRID BIST approach.

c) Novelty and Foundational Character

HYBRID BIST is a complete test solution that, in theory with the right settings, is able to detect both local and global defects accurately. The innovative aspect of this test solution is based on the innovative aspects of the two test solutions on which its operation is based.

Indeed, PETS BIST brings a traditional optical testing aspect, which is more effective in local defect detection than global defect detection. PRED BIST provides a way of testing that is completely decoupled from what currently exists on the ATE and is more effective in global defect detection than local defect detection.

Unlike what already exists in the literature, HYBRID BIST is an integrated optical testing method that is relatively simple considering the coverage of optical tests. Indeed, 100% of the tests will be covered, compared to only a portion covered by test solutions existing in the literature.

III. Impact

The aim of the PhD was to develop and experiment the three BIST solutions on a wide range of sensors: different colours (RGB or monochrome), different resolutions (number of rows and columns), different architectures (number of CMOS transistors inside the pixels) and different technologies (size of the transistors).

The detection of the global and local defects has been used to define whether images are good or bad and, finally if the CIS need to be rejected or not by the BIST solutions. Software emulations of the three BIST engines have been done to validate the test solutions [11][12][15].

Results obtained with our BIST engines shows that, from relatively simple computations used to detect defective images, it allows to sort reliable *PASS* and *FAIL* information for a CIS under test. The optical part of a CIS is tested directly inside the sensor, without any interface that can add sources of errors (potential contact resistance, pad continuity, etc.).

Moreover, using BIST to perform the optical test allows to test each pixel on-the-fly without the need to store a full image before testing as is the case with ATE-based testing. Moreover, BIST is performed at-speed so that test time can be greatly reduced compared with ATE-based test.

Regarding the coverage of optical algorithms usually performed on ATE, we estimate that, by using PETS BIST, more than 50% of these algorithms can be embedded inside the CIS under test, thus leading to a reduction of approximately 30% of the test time for each sensor [11]. This estimation is based on a deep analysis of optical tests, demonstrating that 50% of them usually target local defects and hence can be embedded. The area taken by PETS BIST architecture has been estimated in terms of additionnal logic gates. It represents roughly only 0.25% of the total area of a 1.5 MegaPixels CIS [12].

PRED BIST is bigger because its complexity is higher. It represents 1.5% of the total area of a 1.5 MegaPixels CIS and allows to reduce by 95% the optical test time [15]. Even if PRED BIST is six times bigger than PETS BIST, it allows to cover **all** the optical algorithms performed today with an ATE.

The HYBRID BIST solution leverages the advantages of both BIST approaches presented in [11], [12] and [15] to accurately cover all potential optical defects. Although the results of using HYBRID BIST to perform the optical test of CIS from DB3 are preliminary, they already demonstrate that the impact of this approach can further reduce the number of misclassified images and misclassified sensors when using a test solution directly embedded inside the sensor. These results are promising and will be presented at a future international conference or subjected to a review process.

Although BIST solutions are not perfect, the use of BIST for optical testing of CIS has a significant impact. These three studies open the door to more solutions that could simplify and reduce the impact of optical testing in production on the final cost of CIS.

IV. List of Scientific Outputs

A. List of Papers

- J. Lefevre, P. Debaud, P. Girard and A. Virazel, "A Fast and Low Cost Embedded Test Solution for CMOS Image Sensors," 2021 IEEE International Test Conference (ITC), Anaheim, CA, USA, 2021, pp. 1-9, doi: 10.1109/ITC50571.2021.00007.
  This paper received an Honorable Mention Award.
- J. Lefevre, P. Debaud, P. Girard and A. Virazel, "A Generic Fast and Low Cost BIST Solution for CMOS Image Sensors," 2022 IEEE European Test Symposium (ETS), Barcelona, Spain, 2022, pp. 1-2, doi: 10.1109/ETS54262.2022.9810458.
- J. Lefevre, P. Debaud, P. Girard and A. Virazel, "Predictor BIST: An "All-in-One" Optical Test Solution for CMOS Image Sensors," 2023 IEEE International Test Conference (ITC), Anaheim, CA, USA, 2023, pp. 310-319, doi: 10.1109/ITC51656.2023.00048.

B. List of Posters (National Events)

- J.Lefevre, P.Debaud, P.Girard, A.Virazel, "A Novel BIST Engine for CMOS Image Sensors," *accepted and* *presented at* the national seminar GDR SoC² 2021, Rennes, France.

- J.Lefevre, P.Debaud, P.Girard, A.Virazel, “Configuring a Universal BIST Solution for CMOS Image Sensors,” *accepted and presented at* the national seminar GDR SoC² 2022, Strasbourg, France.

REFERENCES

[1] Standard Test Data Format (STDF) Specification, Version 4, Table of Contents, 2007.

[2] G. Prenat, “Design of an Analog and Mixed-Signal BIST Architecture in Deep Submicron Technology,” PhD dissertation, Institut National Polytechnique de Grenoble, 2005.

[3] J. Chen, “CIS Testing Technology”, Jetek Technology corporation, 2018.

[4] M.Pedersen, J.Y.Hardeberg, “Full-Reference Image Quality Metrics: Classification and Evaluation”, Foundations and Trends® in Computer Graphics and Vision. 7. 1-80. 10.1561/0600000037, 2012.

[5] A.Grochowski, D.Bhattacharya, T.R.Viswanathan, K.Laker, “Integrated Circuit Testing for Quality Assurance in Manufacturing: History, Current Status, and Future Trends”, *in Proc. IEEE Transactions on circuits and systems-II: analog and digital signal processing*, vol. 44, NO.8, 1997.

[6] L. Lizarraga, S. Mir, and G. Sicard, “Experimental Validation of a BIST Technique for CMOS Active Pixel Sensors,” *in Proc. IEEE VLSI Test Symposium*, pp. 189 – 194, 2009.

[7] L. Lizarraga, S. Mir, and G. Sicard, “Evaluation of a BIST Technique for CMOS Imagers,” *in Proc. IEEE Asian Test Symposium*, 2007.

[8] L. Lizarraga, S.Mir, G. Sicard, and A. Bounceur, “Study of a BIST Technique for CMOS Active Pixel Sensors,” *in Proc. IFIP International Conference on Very Large Scale Integration*, pp. 326-331, 2006.

[9] R. Fei, J. Moreau, and S. Mir, “BIST of Interconnection Lines in the Pixel Matrix of CMOS Imagers,” *in Proc. IEEE International Workshop on Advances in Sensors and Interfaces*, pp. 174 –177, 2013.

[10] R. Fei, J. Moreau, S. Mir, A. Marcellin, C. Mandier, E. Huss, G. Palmigiani, P. Vitrou, and T. Droniou, “Horizontal-FPN Fault Coverage Improvement in Production Test of CMOS Imagers,” *in Proc. IEEE VLSI Test Symposium*, pp. 1-6, 2015.

[11] J. Lefevre, P. Debaud, P. Girard and A. Virazel, “A Fast and Low Cost Embedded Test Solution for CMOS Image Sensors,” 2021 IEEE International Test Conference (ITC), Anaheim, CA, USA, 2021, pp. 1-9, doi: 10.1109/ITC50571.2021.00007.

[12] J. Lefevre, P. Debaud, P. Girard and A. Virazel, “A Generic Fast and Low Cost BIST Solution for CMOS Image Sensors,” 2022 IEEE European Test Symposium (ETS), Barcelona, Spain, 2022, pp. 1-2, doi: 10.1109/ETS54262.2022.9810458.

[13] R.Fei. “Alternative Solution to Improve the Production Test of Optical Sensors in CMOS Technology”, PhD dissertation, Grenoble Alpes University, 2015.

[14] C.C. Wan, “CMOS Image Sensors with Multi-Bucket Pixels for Computational Photography”, PhD dissertation, Stanford University, 2011.

[15] J. Lefevre, P. Debaud, P. Girard and A. Virazel, “Predictor BIST: An “All-in-One” Optical Test Solution for CMOS Image Sensors,” 2023 IEEE International Test Conference (ITC), Anaheim, CA, USA, 2023, pp. 310-319, doi: 10.1109/ITC51656.2023.00048.